



Extracting Spatiotemporal Flood Information from News Texts Using Machine Learning for a National Dataset in China

Shengnan Fu¹, David M. Schultz^{2,3}, Heng Lyu¹, Zhonghua Zheng^{2,3}, and Chi Zhang¹

¹School of Infrastructure Engineering, Dalian University of Technology, Dalian, 116024, China

²Centre for Crisis Studies and Mitigation, The University of Manchester, M13 9PL, United Kingdom

³Centre for Atmospheric Science, Department of Earth and Environmental Sciences, The University of Manchester, M13 9PL, United Kingdom

Correspondence: Heng Lyu (lyuheng@dlut.edu.cn)

Abstract. Urban floods present a threat in China, demanding an understanding of their spatiotemporal distribution. Current flood datasets primarily offer provincial-scale insights and lack temporal continuity, which leads to a challenge in detailed analysis. To create a consistent national dataset of flood events, this study introduces a machine learning framework by applying online news media as a primary data source to construct a county-level dataset of urban flood events from 2000 to 2022. Using the Bidirectional Encoder Representations from Transformers (BERT) model, we achieved robust performance in information extraction, with an F1 score of 0.86 and an exact match score of 0.82. Further, a combined model of Bidirectional Long Short-term Memory (BiLSTM) networks with a Conditional Random Field (CRF) layer effectively identified flood locations. Our analysis reveals that the temporal trend of flooded cities in the news-based dataset is similar to the *China Flood and Drought Bulletin*. Furthermore, the consistency of flood events in the news with the typhoon trajectory in two cases, and the connection between flood occurrences and flood conditioning factors, confirm the accuracy of spatial distribution. The validated news-based dataset analyzes urban floods in China from both temporal and spatial perspectives. First, this dataset shows the seasonal characteristics of flood events, which are concentrated in the summer. From 2000 to 2022, the peak year for floods was 2010, and excluding the influence of peak year, the overall temporal trend of total flood occurrence shows an increase. Spatially, the distribution of floods decreases from southeast to northwest, with Guangxi Province having the highest number of floods. Additionally, the Yangtze and Pearl River basins are most frequently affected by urban floods. The subtropical climate zone is the most susceptible to flooding. This study provides an automated and effective method for constructing a national flood event dataset and reveals the spatiotemporal characteristics of urban flooding in China.

1 Introduction

Floods have been a recurring challenge in China throughout its history, with efforts to manage them spanning four millennia (Feng et al., 2023; Jiang et al., 2023). Cao et al. (2022) found that China and the United States were the two countries with the highest urban flood exposure, together accounting for approximately 61.5% of the global increase in urban flood exposure. In China, more than three urban flooding events happened annually in 137 cities from 2008 to 2010 (Zhang et al., 2018). In recent years, Zhengzhou had torrential rainfall and subsequent flooding on 21 July 2021, resulting in 380 deaths and direct economic



losses of 168 billion dollars (Dong et al., 2022). In another example, Shenzhen experienced short-duration and extremely heavy
25 precipitation on 11 April 2019, leading to floods and 11 deaths (Zhang et al., 2023c). Thus, urban flooding is an important risk
factor affecting urban property and public safety in China.

To develop more targeted strategies to mitigate flood damage, understanding the historical urban flood distribution is crucial.
Analyzing the temporal and spatial distribution of floods helps in identifying flood-prone areas. By analyzing the climate and
geographical features of flood-prone regions, what causes the floods can be discovered, leading to possible flood-control strate-
30 gies (Ahemaitihali and Dong, 2022; Zhang et al., 2023a). Previous studies about the distribution of floods has demonstrated
the reliance on the historical flood datasets (Zhao et al., 2018; Wu et al., 2019; Xu and Tang, 2021).

Although having a database of floods in China is desirable, no single dataset provides comprehensive information about
floods at a scale smaller than the provincial level in China. The existing official Chinese datasets are summarized in Table 1.
However, each of these datasets have their own specific applicability and limitations in different scopes. Notably, the *Annual*
35 *Report of Chinese Hydrology* is more suitable for basin flooding studies than urban flooding, and it only began publication
in 2021. The *China Flood and Drought Bulletin* lists both urban flooding and basin flooding information but only offers the
spatial distribution of accumulated disaster data at a provincial scale since 2006. The *China Meteorological Disaster Yearbook*
only includes records of severe events that result in significant losses, leading to a smaller number of records of the more
frequent urban floods that cause minor damage. Additionally, the information on the website of the China National Disaster
40 Reduction Center is relatively detailed and similar to news reports, as both are documented at the time of disaster occurrence.
However, the data collected before 2018 became inaccessible due to a change in the website that followed the creation of the
Emergency Management Department of China in 2018.

In addition to the official Chinese datasets, there are also several natural disaster datasets recording flood events created by
other governments or organizations (Table 2). Each dataset has a different research perspective, which makes it impossible to
45 create a long-term statistical analysis of historical urban floods in China. The Emergency Events Database (EM-DAT) includes
detailed information on global disaster events, such as timing, location, and losses, but it only includes severe events that cause
damage of a certain scale. The *Natural Disaster Data Book* published by the Asian Disaster Reduction Center is an analysis
of EM-DAT data specifically for the Asian region. The Dartmouth Flood Observatory focuses on global flood events, offering
more detailed information with locations pinpointed to latitude and longitude. However, its records in China are insufficient,
50 with the total number of flood events recorded from 1985 to the present not exceeding 400 cases. Additionally, both the
Copernicus Emergency Management Service and the Global Flood Monitoring System are based on real-time satellite data
monitoring, which is more suitable for flood forecasting or real-time inundation progression simulation than historical flood
statistical analysis.

The existing datasets clearly show that there are gaps in the urban flood records, lacking continuous records at a finer spatial
55 resolution, such as at the county or neighborhood level. However, given that China has a land area of approximately 9.6 million
square kilometers (Zhang et al., 2023b), the provincial or prefecture-level administrative regions typically cover large areas
that contain diverse meteorological and geographical characteristics (Wang et al., 2013; Shang et al., 2023). This diversity may
lead to bias in the studies on comparing the flood characteristics of different cities in the same province or analyzing the flood



causes. In contrast, county-level administrative divisions narrow down the scope, offering a more homogeneous perspective
60 that could improve the accuracy of such flood datasets. Therefore, a continuously updated national urban flood dataset on a
county level that includes records covering at least the past 20 years should be built to bridge the gap.

For the urban flood dataset construction, researchers often supplement governmental data with remote-sensing imagery
(Huang and Jin, 2020; Shahabi et al., 2020) and field-survey data (Eini et al., 2020; Darabi et al., 2021). Remote-sensing
images offer the potential to infer the progression of disasters, but information retrieval through remote sensing is plagued by
65 uncertainties due to factors such as cloud cover (Datla et al., 2010; Donovan et al., 2019). On the other hand, field surveys
provide highly accurate, first-hand data. However, the process is both time-consuming and labor-intensive (Surampudi and
Yarrakula, 2020; Feng et al., 2022), making it challenging to support the collection of historical flood events on a large scale.
Given these limitations, selecting proper data sources and related processing techniques to collect national urban flood records
remains a challenge.

70 Against this backdrop, digital news media data emerges as a promising alternative. News data offers timely, authentic, and
extensive coverage of disaster events (Williamson, 2019; Antwi et al., 2022). Moreover, media coverage tends to focus on the
current impact of disasters on humans, infrastructure, and the environment, and on the regions related to the events (Houston
et al., 2012), which are exactly the elements needed to construct a disaster dataset. Some studies about natural hazards have
revealed the power of media data to supplement the shortcomings of traditional natural science data sources (Avellaneda
75 et al., 2020; Lai et al., 2022). For instance, Yang et al. (2023) analyzed the clustering of multiple natural disasters including
earthquakes, floods, droughts, etc. in China based on news data. Similarly, Liu et al. (2018) used news media data to extract
characteristics of natural disasters, uncovering a significant coexistence of meteorological and geological disasters. Our study
would extend these efforts by developing a county-level historical flood database based on news data, focusing on urban floods.

To extract flood events from news data, event extraction techniques in the field of natural language processing can offer
80 support (Xiang and Wang, 2019; Olivetti et al., 2020). Early event extraction approaches based on pattern matching (Bui et al.,
2013) have given way to machine learning models that can automatically extract semantic features, offering more nuanced
understanding and flexibility in handling diverse event types (Sha et al., 2016; Liu et al., 2020). Some researchers have proposed
machine reading comprehension methods (He et al., 2018; Farooq et al., 2020), achieving event extraction in a question-answer
format, which can effectively generalize to previously unlabeled event types.

85 The innovative application of the question-answer format offers an advancement over using solely Named Entity Recognition
(NER) methods for identifying the locations of flood disasters. The NER is an information extraction method for finding
and sorting named entities into pre-defined tags (persons, locations, and organizations). It can automatically extract place
names from texts by analyzing the structure and grammar of sentences. Previous studies on disaster information extraction
commonly adopted NER methods such as the bidirectional long short-term memory network (BiLSTM) combined with a
90 Conditional Random Field (CRF) layer, which were trained with a large number of place name tags (Kundzewicz et al., 2019;
Yan et al., 2024). The NER methods identify all place names in the text regardless of their contextual background, leading to
the recognition of place names not related to the flood disaster. For instance, in the sentence “Many volunteers from Beijing
went to the disaster area in Shanghai”, “Beijing” is not a disaster-affected location, but it would still be output by the NER



model as a result. In contrast, the question-answer model could distinguish between disaster-affected and unaffected areas
95 by posing targeted questions (Sun et al., 2021; Zhang and Zhang, 2023). Currently, the best-performing machine reading
comprehension models are pre-trained language models (Yoon et al., 2019; Li et al., 2021). The pre-trained models capture
deep semantic relationships between sentences through extensive semi-supervised training on a large corpus, achieving an
accurate understanding of contextual information, thereby completing question-answering tasks.

Among the pre-trained models, the Bidirectional Encoder Representations from Transformers (BERT) (Devlin et al., 2018)
100 is a seminal model which has proven to be effective and widely adopted. The strength of the BERT model lies in the innovative
use of bidirectional pre-training on large-scale unlabeled text data like Wikipedia and books, allowing it to be effective for
information extraction across diverse fields (Xiong, 2020; Suwaileh et al., 2020). Some cases illustrate the accuracy of BERT
in identifying events from unstructured text, identifying speech for transcription, and building a question-answer system with
a small number of samples (Wang et al., 2021; Huang et al., 2021). These successful applications show the potential of BERT
105 to identify the flood events information from news text data.

The capabilities of the language model, combined with the reliability of news data, provide us with an opportunity to
construct a new flood event datasets to address the absence of datasets at the county level. Therefore, this present study
aims to develop a national county-level urban flood dataset from 2000–2022 based on news data through a machine learning
framework. The performance of the BERT model in the field of flood disaster knowledge is examined and the spatiotemporal
110 characteristics of urban floods in China based on news records are analyzed.

The remainder of this paper is organized as follows: Section 2 introduces the data used including a Chinese text dataset
used to train the BERT model, as well as news data and validation data. Section 3 describes the processes of flood information
extraction by the BERT model and flood location recognition using a BiLSTM network combined with a CRF layer. Section
4 shows the performance of the BERT model, as well as the accuracy evaluation of extracted flood information and the spa-
115 tiotemporal distribution of the flood information. Section 5 discusses the findings and limitations of the study. Finally, Section
6 outlines the summary of our key contributions and results.

2 Data Preparation

Three kinds of datasets were used in this study. Section 2.1 describes a Chinese machine reading comprehension data called
CMRC2018 (Cui et al., 2018) used to train the BERT model. Section 2.2 explains the news data used to extract information on
120 urban flooding. Section 2.3 interprets the validation data selected to assess whether the extracted flood information is accurate.

2.1 CMRC2018

The CMRC2018 dataset is a span extraction dataset for Chinese machine reading comprehension, consisting of nearly 20000
real-world questions annotated by human experts on Wikipedia paragraphs. The task of reading comprehension is to obtain
the corresponding answer from the given context and question, and span extraction indicates that the content of the answer is
125 all in the context, and the length of the span is determined by the distance between the start and end positions of the answer.



Table 1. Summary of official flood disaster statistics reports

Name	Period	Flood Records	Update Frequency	Source
<i>Annual Report of Chinese Hydrology</i>	2021–	Records of basin/river floods in various provinces and cities	Annual	Ministry of Water Resources of the People’s Republic of China
<i>China Flood and Drought Bulletin</i>	2006–	The flood disaster situations in various provinces include population, economic, and crop losses	Annual	Ministry of Water Resources of the People’s Republic of China
<i>China Meteorological Disaster Yearbook</i>	2004–	Record criteria as events causing over 50,000 hectares of agricultural damage, 10 deaths, or 14 million USD in direct economic losses	Annual	China Meteorological Administration
Reports on official website of China National Disaster Reduction Center	2011–	Detailed records of the time, location and damage of flood events (Data prior to 2018 is not available)	Real-time	National Disaster Reduction Center of China

The dataset used in this study contains 2282 training samples. Each sample consists of a group (C, Q, A), where C represents context, Q represents questions, and A represents answers. The answer to each question should be a span extracted from context. Figure 1 shows an example including a context describing a model’s resume, as well as a question about the content of the context and the corresponding answer. In this study, the CMRC2018 dataset was used to fine-tune the BERT model to adapt to the Chinese machine reading comprehension task.



Table 2. Summary of global natural disaster datasets

Name	Period	Flood Records	Update Frequency	Source
The Emergency Events Database (EM-DAT)	1900–	Time, location and damage of global flood events that resulted in a certain number of deaths or economic losses	Annual	Centre for Research on the Epidemiology of Disasters
<i>Natural Disaster Data Book</i>	2002–	Statistical and analytical perspectives of flood events in Asia (data retrieved from EM-DAT)	Annual	Asian Disaster Reduction Center
Dartmouth Flood Observatory (DFO)	1985–	Time, location and extent of global flood events using satellite observations	Continuously but irregularly updated	University of Colorado Boulder
Copernicus Emergency Management Service (CEMS)	Real-time	Ongoing and upcoming flood events information from satellites to support flood forecasting at national, regional and global levels	Real-time	European Union Copernicus Programme
Global Flood Monitoring System (GFMS)	Real-time	Flood inundation extent and depth based on precipitation satellite data and flood model simulation	Every 3 hours	University of Maryland and NASA

2.2 News Data

The news used in this study was collected from two Chinese newspaper databases covering the whole of China, including WiseNews (<https://wiseneeds.wiseneeds.net/>) and the newspaper database of the China National Knowledge Infrastructure (CNKI) website (<https://navi.cnki.net/knavi/newspapers/index>). WiseNews is a full-text news database that provides access to more than 600 newspapers, magazines, and websites from China. Its news coverage dates back to 1998 and is updated daily to the present. The CNKI database is sourced from more than 500 important newspapers in China covering the period from 2000 to the present. The main difference between these two databases is that CNKI has certain selection criteria for selecting academic and informative documents and therefore returns different amounts of results for the same searching keywords. The newspaper sources collected by the WiseNews database could cover the newspaper sources collected by CNKI.



[Context]

Anya Russell is a model from St. Petersburg, Russia. She was the runner-up of the 10th season of the American Super Model Rookie Contest. At the age of 17, Anya participated in informal fashion shows for brands such as Chanel, Louis Vuitton, and Fendi. Anya said during the semi-finals interview that she is passionate about the modeling industry, so she participated in the American Super Model Rookie Competition. She performed outstandingly in the competition, having been nominated for first place five times and achieving her best performance ever (2.64) in average order

[Question]

What competition did Anya Russell participate in and win the runner-up?

[Answer]

Season 10 of the American Super Model Rookie Contest

Figure 1. An example in CMRC dataset.

140 CNKI was selected as the primary source to manually extract the spatiotemporal information of the floods due to its high concentration of academic and informative content. In total, 2730 pieces of news from 2000–2021 were collected by setting the keywords of the subject as (“flood” OR “flood disaster”) and the keywords in any full text as (“city” OR “county” OR “district”). After a manual review to remove duplicates and irrelevant entries, including those referring to flash floods which occur suddenly in mountainous areas and are not the focus of this study, the final dataset consisted of 253 relevant news articles.

145 These relevant news articles were then segmented into paragraphs and reorganized into 633 distinct samples. Among them, 503 samples were used to fine-tune the BERT model, alongside data from the CMRC2018 dataset, enhancing the model’s ability to accurately extract flood disaster information. The remaining 130 samples served as a test set to evaluate the model’s performance.

Building on the method successfully applied to CNKI data, the WiseNews database subsequently employed the fine-tuned
150 BERT model for analyzing flood-related news. To refine the search and improve data quality, terms “floods and beasts” and “flash flood” were excluded due to their tendency to retrieve unrelated news based on the experience of processing CNKI news data. “Floods and beasts” is an idiom in Chinese, which is often used as a metaphor for frightening things. This idiom contains the word “flood”, so some unrelated news items that used it to describe other disasters or bad phenomena may be included in the search results. Therefore, the refined search strategy used was (“flood” OR “flood disaster”) AND (“city” OR “county” OR



155 “district”) NOT (“flash flood” OR “floods and beasts”). This search returned a total of 46118 news items, with a time frame from 2000–2022.

2.3 Validation Data

The *China Flood and Drought Bulletin* (Table 1) was used to assess the accuracy of flood events reported in news texts. Although these bulletins provide annual flood event and loss data at the provincial level, they are not directly comparable with
160 the county-level flood information derived from news sources in this study. However, bulletins from 2006 to 2018 include data on the number of cities affected by floods, which were used to verify the city-level flood occurrences identified in this study.

To further evaluate the spatial accuracy of flood event reporting, this study analyzed the coverage of typhoon-related urban flooding events during two specific typhoon periods. Stronger typhoons tend to cause more extreme rainfall, which leads to urban flooding (Chan et al., 2021; Liu et al., 2021). If the flood-affected areas reported in the news are consistent with the
165 typhoon trajectories and potential impact areas, this correlation would confirm the spatial accuracy of the news-based flood data. The typhoon path and intensity information used in this study were sourced from the National Institute of Informatics (NII) in Japan (<https://kaken.nii.ac.jp/>).

Additionally, this present study selected two primary flood conditioning factors that quantify topography and precipitation to evaluate the characteristics of news-derived flood distribution. According to hydrological research, areas with more precip-
170 itation and lower-lying topography are more prone to urban flooding (Guo et al., 2021; Chen et al., 2023; Wang et al., 2019). If the flood locations identified from news reports tend to have higher precipitation levels and are concentrated in lower-lying areas, this would be consistent with established hydrological principles. In this study, the average daily precipitation from 2000 to 2022 for each county was calculated based on the ERA5-Land dataset. Topography was quantified using elevation data (Zhu et al., 2023) from the Shuttle Radar Topography Mission (SRTM) with a 90-meter grid spacing.

175 3 Methods

In this study, a machine learning framework was adopted to extract spatiotemporal flood event information from news texts. Section 3.1 describes how flood information was extracted from related news texts using BERT model through a question-answer format. Section 3.2 shows the flood location recognition methods based on a NER model. The overview of the framework is illustrated in Figure 2.

180 3.1 Flood Information Extraction

The BERT machine reading comprehension technique was used to extract the time and location of the disaster from news texts. Section 3.1.1 introduces the data preparation and Section 3.1.2 presents the BERT model construction and application. Section 3.1.3 explains the evaluation metrics for model performance.

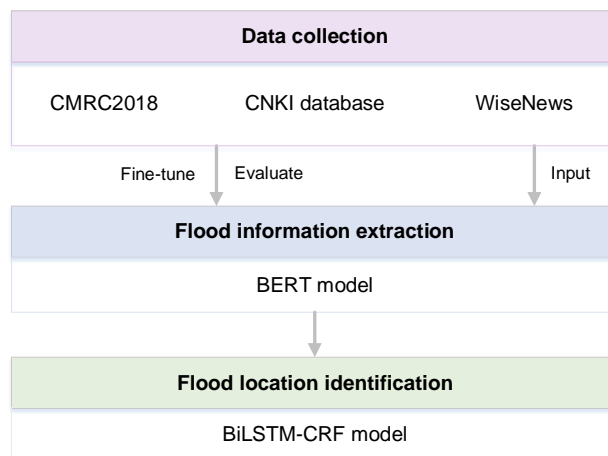


Figure 2. The framework of flood information collection and extraction.

3.1.1 Data Preparation

185 Data pre-processing in this study included both data cleaning and splitting. Initially, news documents downloaded from the database contained extra characters such as copyright information, news web links, and numerous empty lines, which were irrelevant to the news content. These irrelevant content was efficiently removed using the regular expression (“re”) module in Python. Moreover, given that news documents can be lengthy and may exceed the input length limitations of the BERT model, each news text was divided into multiple samples.

190 After pre-processing, flood news texts were manually annotated to align with the CMRC2018 data format. For the training samples, the content of each news article was labeled as the context, and three questions were proposed per context, addressing the flood information. The questions included the following “Question 1: What natural disaster occurred? Question 2: When did the disaster occur? Question 3: Where was the disaster located?” Answers were manually annotated based on the news content. Finally, 503 samples from CNKI news were formatted into a training set, of which 80% were combined with the
195 CMRC2018 dataset to fine-tune the model, while the remaining 20% of the samples were used as a validation set to adjust hyperparameters. The remaining CNKI samples and all the WiseNews samples were processed into test samples mirroring the training sample format, except that the answers were not annotated. For the CNKI test samples, the answers generated by the model were also manually evaluated to assess the accuracy. Once the model’s efficacy was confirmed through these assessments, it was subsequently applied to the WiseNews samples.

200 3.1.2 BERT Model Construction and Application

BERT, which is designed to pre-train deep bidirectional representations from large unlabeled data sets (Devlin et al., 2018), was introduced to extract flood information in this study. The model structure is a multi-layer bidirectional transformer encoder,



which is an attention mechanism that learns contextual relations between words. Unlike other traditional bidirectional language models where the contextual representation of each token is a concatenation of the forward and reverse representations, the transformer encoder reads the entire sequence of words at once. There are two procedures for constructing a BERT model: 205 pre-training and fine-tuning.

For pre-training, the model is trained on unlabeled text data using two unsupervised training strategies. First, BERT proposes a masked language model, inspired by the cloze task (Taylor, 1953), in which 15% of the input tokens are randomly masked by a special label [mask], and these masked tokens are then predicted. Secondly, BERT adopts next-sentence prediction into the 210 training process. A binary next-sentence prediction task is pre-trained to enable the model capable of understanding sentence relations. The model takes in pairs of sentences as input and attempts to identify if the second sentence within the input pair is the subsequent one in the original context.

Following pre-training, the downstream task for fine-tuning in this study involves extracting answers from the context based on posed questions. In typical applications, BERT models predict where answers start and end in a text by adding a classification 215 layer known as softmax. The process begins with tokenization, where the text is divided into smaller units called tokens, which can represent words, phrases, or punctuation marks. Then, the model calculates the probability of each token being the start and end of the answer, separately. This allows the model to identify a continuous text fragment as the answer, which is suited for scenarios where a single optimal answer is required. However, the locations affected by a flood event are generally not unique, and the descriptions of multiple disaster areas in the news may be scattered in discontinuous statements. This requires 220 a method that can extract multiple answers for our study.

To enhance the model's ability to manage multiple answers, a BIEO (Beginning, Inside, End, Outside) tagging layer is integrated into the input (Li et al., 2019). This modification enables the model to predict one of four possible tags for each token: "Beginning" for the starting token of an answer, "Inside" for intermediate tokens within an answer, "End" for the final 225 token of an answer, and "Outside" for tokens that do not form part of the answer. This approach allows the model to recognize multiple independent answer fragments within a paragraph, since each answer fragment is marked by an explicit start and end and connected by an intermediate tag. This enhanced capability makes the model exceptionally suitable for complex, multi-answer scenarios like analyzing fragmented disaster reports. Figure 3 shows the overall structure of the model used in this present study. Here, the context and query processed through the BIEO tagging layer, and their semantic information is learned via the BERT structure. Finally, the probabilities that each token belongs to BIEO of the answer are determined through a linear 230 layer and softmax function. The BERT-base model was fine-tuned for three epochs with a learning rate of 5×10^{-5} and a batch size of 8, which were determined to be the most effective combination among the tested settings. Results of other combinations can be found in Table A1 in Appendix.

To build the set of urban flooding events, the output of the BERT model needs to be further confirmed and collated. The first step was to check whether the news contained a flooding event. If the answer to Question 1, "What disaster happened," contains 235 the keywords "flood" or "flood disaster" and does not contain the words "will," which indicates the forecast, the news sample is considered to describe a flood disaster event. As the long text news was split into different samples in the pre-processing procedure, the news could be confirmed as long as one of the answers of multiple samples belonging to the same news met the



conditions. For time information, once the answer to Question 1 was confirmed to be a flood event, then the answer to Question 2 was the time of the flood, and the year information is the year of the news release if the answer did not include the year.
 240 For location information, similar to confirming time information, if the answer to Question 1 is confirmed, then the answer to Question 3 contains the flood locations.

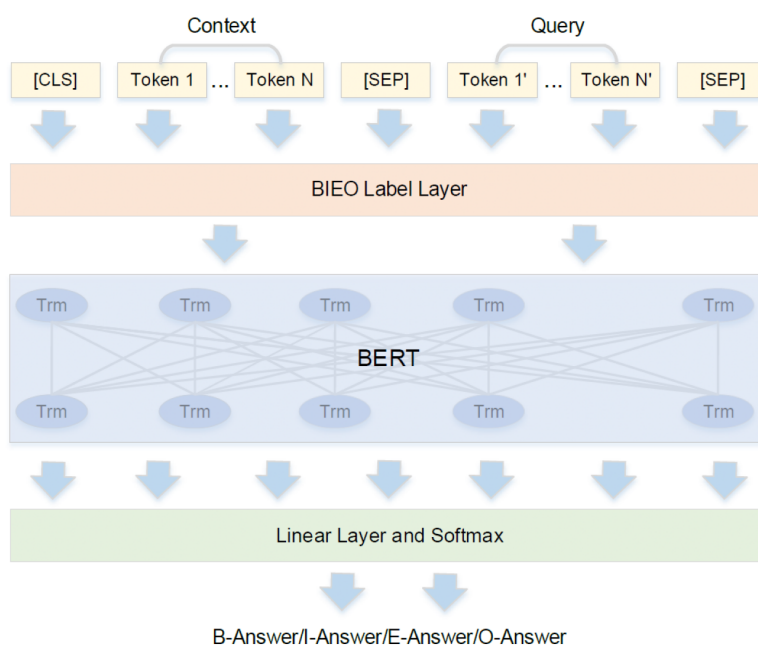


Figure 3. The structure of the BERT model proposed in this study. [CLS] and [SEP] are special markers that identify the beginning and end of the input text. [CLS] stands for “classification”, and adding a [CLS] token at the beginning of the input text allows the model to learn a representation for the whole sentence. [SEP] stands for “separator”, used mainly to separate different sentences or pieces of text. The Trm inside BERT represents the transformer architecture.

3.1.3 Evaluation metrics

In this study, two evaluation metrics were used to assess the effectiveness of flood information extraction. These metrics are common across a number of disciplines, yet use different names (Brooks et al., 2024). Initially, the identification of flood events
 245 was treated as a classification problem, using precision, recall, and the F1 score to evaluate the accuracy of predictions. The metrics were calculated as:

$$Precision = \frac{TP}{TP + FP} \quad (1)$$

$$Recall = \frac{TP}{TP + FN} \quad (2)$$



250

$$F1_{score} = \frac{2 \times Precision \times Recall}{Precision + Recall} \quad (3)$$

For the computation of these indexes, Table 3 explains the classification outcomes in terms of True Positives (TP), False Positives (FP), False Negatives (FN), and True Negatives (TN). Among the metrics, precision is defined as the ratio of correctly predicted flood news to all predictions labeled as flood events. Recall measures the proportion of correctly predicted flood news out of all actual flood events. F1 score combines precision and recall scores as the harmonic mean, providing a balanced view of the model's performance. A higher F1 score indicates superior model performance.

Table 3. Classification outcomes for flood identification

True Condition	Prediction Result	Label
Flood	Flood	True Positive (TP)
Flood	Non-flood	False Negative (FN)
Non-flood	Flood	False Positive (FP)
Non-flood	Non-flood	True Negative (TN)

Furthermore, for the extraction of flood event information, two matching criteria were applied (Rajpurkar et al., 2016). The first index is called exact match, which measures the matching degree between the prediction and ground truths. The score is 1 for the EM of both the time and location information extracted. Otherwise, the score is 0. There is usually more than one disaster location in one flood event and maybe the model can output several but not completely accurate locations. Therefore, a fuzzy match was used to evaluate the location extraction using precision, recall, and F1 score. Unlike the classical formula, the precision and recall were calculated as:

$$Precision = \frac{P}{M} \quad (4)$$

$$Recall = \frac{P}{N} \quad (5)$$

Where P represents the number of accurately extracted flood locations, M is the total number of predicted flood locations and N is the total number of actual flood locations observed in the texts. The F1 score was computed using the classical formula as Equation 3, providing a balanced view of the quality and completeness of the predicted locations.

3.2 Flood Location Recognition

In most flood location answers, there is not only the name of the place itself but also the characters before or after it (e.g., “it occurred in Hangzhou”). Therefore, a BiLSTM-CRF model was adopted to further extract the place names from the answers.



The model was trained on the Microsoft Research Asia corpus, which is an available data set for the Chinese NER. The characters in the Microsoft Research Asia corpus were tagged as named entities representing persons, locations, and organizations. The model framework used in this present study is detailed in Fu et al. (2022).

275 After identifying the flood locations, it was essential to verify and revise the list of places in accordance with the latest national administrative divisions. This involved updating any names of districts or counties that had been renamed to reflect the most current terminology. After that, flood locations were matched with the administrative division shape file and visualized using ArcGIS.

4 Results

280 The results section consists of three primary parts: Section 4.1 evaluates the BERT model's performance using different metrics. Section 4.2 shows the accuracy of the number and spatial distribution of floods extracted from news using different categories of validation data. Section 4.3 presents the content of the urban flood dataset constructed, highlighting both the temporal distribution in the volume of related news articles and flood events and the spatial distribution of floods across county regions, as well as various basin and climate zones.

285 4.1 The performance of the BERT model

The effectiveness of flood-event recognition and flood-information extraction is presented in Table 4. The BERT model demonstrates excellent performance in identifying whether an event is a flood, achieving an impressive F1 score of 0.98. On the other hand, the overall performance of flood-information extraction is satisfactory, with an F1 score of 0.86 for location extraction and an EM of 0.82 for both time and location extraction. The high F1-score and EM values (over 0.80) demonstrate that integrating domain-specific knowledge enabled the model to respond to questions about flood information.

Table 4. The performance of the BERT model (EM index was not applied to evaluate event identification)

	Precision	Recall	F1-score	EM
Flood-event identification	0.98	0.98	0.98	N/A
Flood-information extraction	0.96	0.78	0.86	0.82

290

4.2 Accuracy evaluation of the flood information

To validate the news-based flood dataset, a comparative analysis was conducted using records from the *China Flood and Drought Bulletin*. The comparison of annual flooded cities from the *China Flood and Drought Bulletin* with those identified in news sources between 2006 and 2018 is displayed in Figure 4. Detailed yearly comparisons are summarized in Table A2 in
295 Appendix. The similarity between these time series indicates that the news-based method provides a reasonable approximation



of historical flood-event records. However, the difference also suggests a bias, especially in the years that experienced peak flood occurrences.

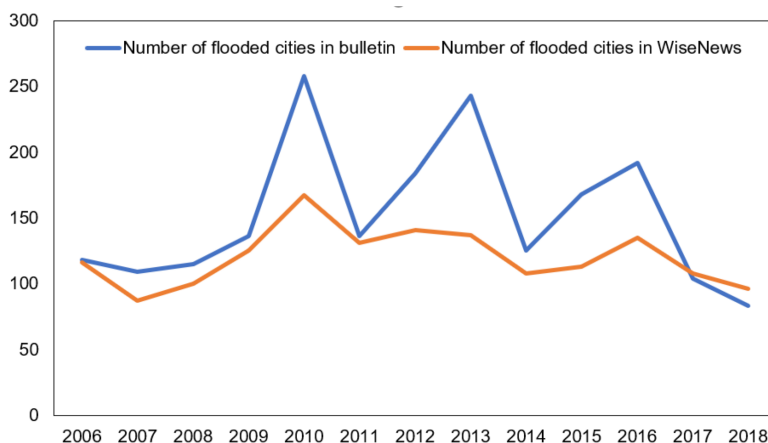


Figure 4. The comparison between the time series of number of flooded cities extracted from news and *China Flood and Drought Bulletin* for each year.

The bias between news-based flood data and the *China Flood and Drought Bulletin* may be attributed to media attention. The news-derived flood distribution was compared with regional Gross Domestic Product (GDP) distribution to assess whether economic development introduces a bias in media attention. By clustering the regional GDPs of each county using the K-means method, all counties were classified to 3 groups. Figure 5 presents the box of normalized flood occurrence and GDP values for each group, which reveals a trend of higher GDP regions reporting more flood events. This trend suggests that economic development influences media coverage and public attention. The research by Lu et al. (2022) also indicates that economically developed and urbanized cities receive more media attention. Additionally, media attention towards urban floods is often driven by the severity of the events. For example, Anhui with low media coverage has experienced huge cumulative economic losses from floods in the *China Flood and Drought Bulletin* over the years. This lack of attention is not due to single disaster, but rather a series of smaller floods affecting the area. This selective reporting leads to a lower occurrence in news-based dataset than the *China Flood and Drought Bulletin*.

Consider that the bias sourced from media coverage may also affect the spatial distribution of floods, the subsequent analysis focuses on verifying the accuracy of spatial distribution. Due to the lack of direct spatial distribution information on floods at the county level across China, two kinds of indirect data proven to have certain relationships with flood events, have been investigated. First, this present study focused on a targeted verification of the news extraction method by examining its performance during two severe typhoon events. The reason for selecting Typhoons Lekima and In-fa is that both events caused severe economic losses and casualties and had an extensive spatial impact, spanning multiple provinces. Typhoon Lekima, a super tropical cyclone that originated from the Western North Pacific in 2019, was one of the costliest natural disasters in China, causing 14 million victims with at least 71 deaths and costing 9.22 billion dollars in damages (Qi et al., 2021). It made landfall

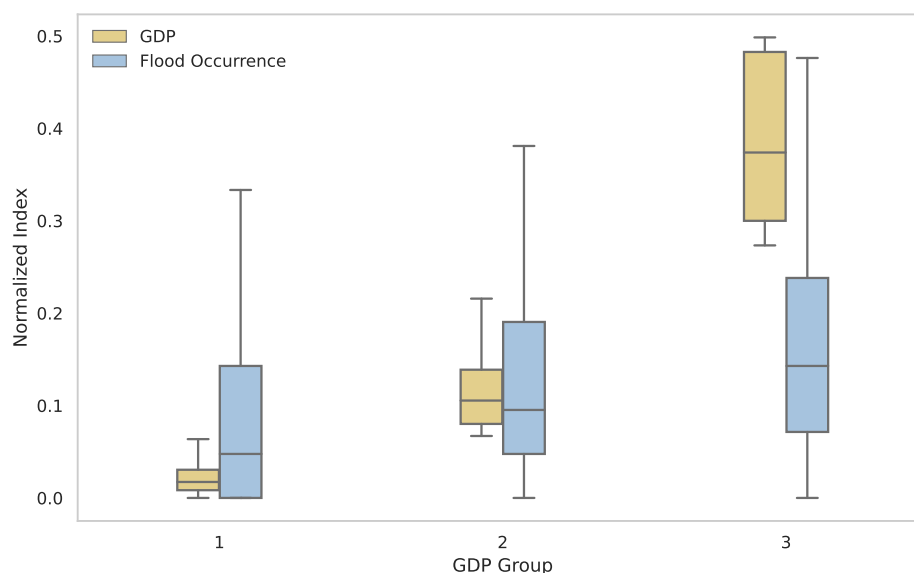


Figure 5. The box of flood occurrence and GDP by GDP groups. The vertical axis shows the value after normalizing GDP and flood occurrence between 0 and 1.

in Wenling, Zhejiang Province, on 10 August, then slowly moved north along China's east coast, making a second landfall in Qingdao, Shandong Province, on 11 August, before finally dissipating in the Bohai Gulf on 13 August (Zhou et al., 2022). This typhoon lingered over the land for 44 hours, causing heavy rainfall in many areas, particularly in Shandong where the maximum accumulated rainfall exceeded 400mm (Gao et al., 2023). Figure 6a shows the route of Lekima, along with flood events extracted from the news during the typhoon's progression. The flood locations between 10 and 13 August were closely dispersed on both sides of the Lekima's trajectory, and the sequence of occurrence was also consistent with the time of the typhoon trajectory. Another typhoon in 2021, called In-Fa, also demonstrated this consistency, as shown in Figure 6b. On 25 July, Typhoon In-fa made landfall in Zhoushan, Zhejiang. On 26 July, it made a second landfall in Pinghu, Zhejiang, then gradually moved northward, weakening into a moderate cyclone, and was dissipated on 30 July. The flood locations reported in the news during the typhoon's movement were consistent with the route of In-Fa. These findings indicate the effectiveness of the news-based method in capturing the distribution of flood events in the aftermath of major storms.

Another indirect evaluation of the spatial distribution of flood events at the county level across China was exploring the relationship between flood occurrence and flood conditioning factors, including precipitation and elevation. Precipitation is a direct contributor to urban floods and heavy rain leads to surface water accumulation. Elevation influences how water flows and accumulates in an area, with lower areas more prone to flooding after heavy rains due to water flowing downward. In this study, the average daily precipitation from 2000 to 2022, derived from the precipitation grids within each county-level administrative boundary, was selected. Figure 7 displays the distribution of elevation and precipitation for flood-affected locations extracted in this study. The intensity of the data points' color reflects the total number of flooding events at those locations, with darker col-

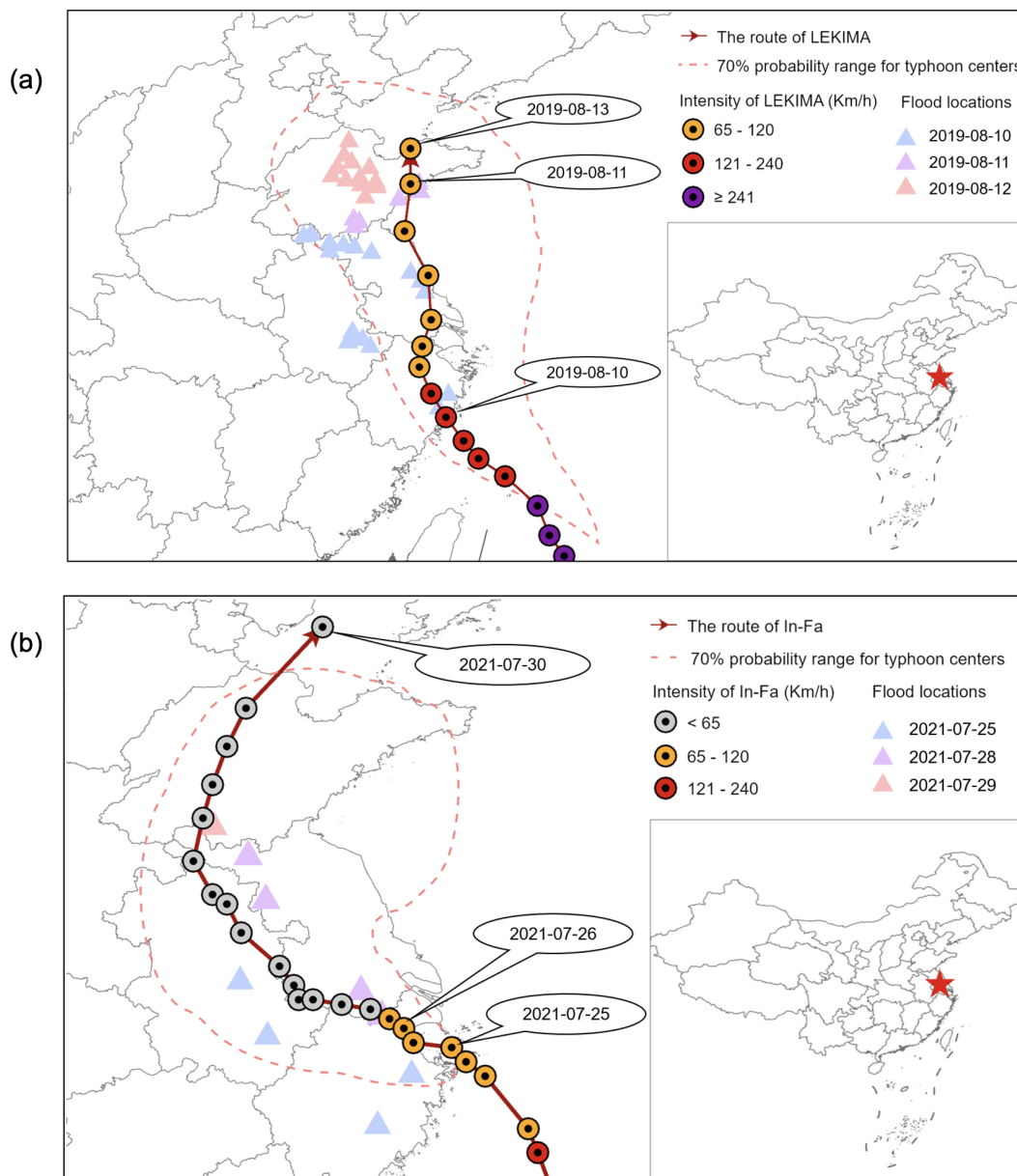


Figure 6. The typhoon routes and related flood locations. The red solid line in the figure represents the actual path of the typhoon movement, while the range within the dashed line is the range of the typhoon center predicted at the beginning of the typhoon landing, and the forecast accuracy is 70% probability. (a) Typhoon Lekima; (b) Typhoon In-Fa.

335 ors denoting a higher occurrence. The points with darker colors, which correspond to high-occurrence flood-affected locations, are predominantly situated in areas of higher precipitation and lower elevation. The spatial distribution of news-sourced floods is concentrated in these highly sensitive areas, demonstrating consistency with established hydrological principles. Despite the



systematic bias caused by media attention, two indirect validation methods above indicate that the spatial distribution of floods extracted from the news is reasonably accurate.

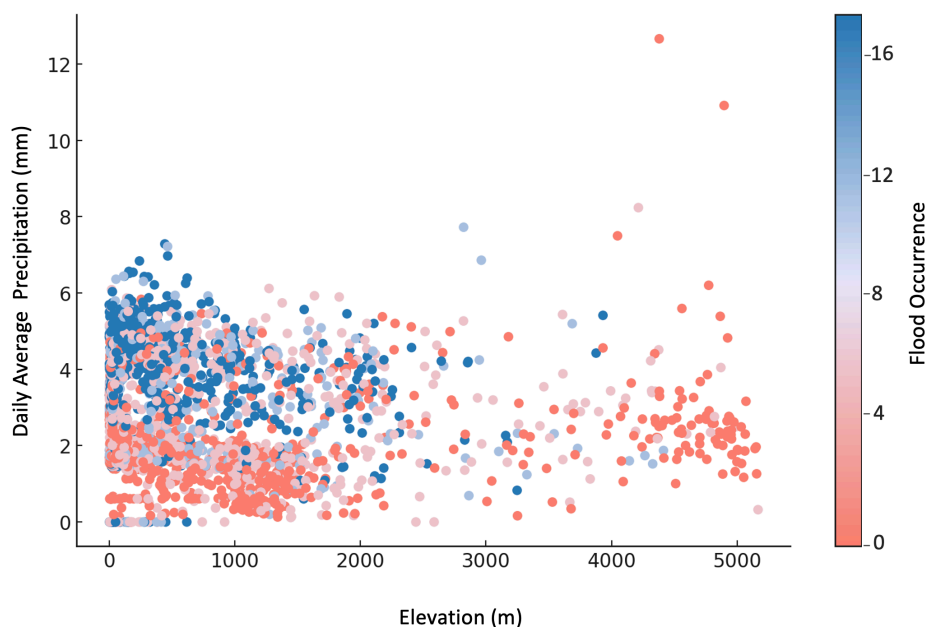


Figure 7. The distribution of daily average precipitation and elevation of each county and related flood occurrence. The x-axis and y-axis show the elevation and precipitation values for each county, respectively, and the color of the dots shows the corresponding number of flood occurrence for each county according to the color scale.

340 4.3 The urban flood dataset

After using a mixed strategy on the accuracy evaluation of the news-based flood information, this section introduces the temporal and spatial distributions of the verified national urban flood dataset. The dataset records urban flood events reported in news articles from 2000 to 2022, including the timing of these events at the monthly level and the affected areas at the county level. Currently, the dataset records a total of 2048 counties affected by flood disasters during these years, with a total
345 occurrence of 7559 times. Section 4.3.1 presents the temporal distribution, which shows the monthly changes in the number of news articles about urban floods and the number of flood events in county-level regions. Section 4.3.2 shows the spatial distribution of the total number of floods in county-level regions, along with the trend of floods across different basins and climate zones.



4.3.1 Temporal distribution of flood events

350 Figure 8 shows the temporal distribution of historical flood locations in China from 2000 to 2022. It displays the flood occurrence each month of every year, with darker colors indicating more frequent floods. The comparison of monthly flood occurrences across different years shows little variation, which reveals an evident seasonal cycle. The summer months (June–August) experienced a higher occurrence of flooding, accounting for 74% of total flooding events. In contrast, the winter season (December–February) which recorded few flood events, only accounted for 1%. This is impacted by the climate’s tendency for
355 precipitation to be concentrated in the summer. The seasonal characteristics are consistent with the findings of Xu and Tang (2021)’s analysis of multi-disaster data from 2011 to 2019 in China, which showed that floods predominantly occurred from April to September, with the highest frequency in July. Our study found June to be the most frequent month for floods, possibly due to the different study periods.

Over these years, the total number of flood events per year did not show a continuous increase but rather a rise and fall, with a
360 peak in 2010. This pattern is consistent with the trends observed in the *China Flood and Drought Bulletin* (Figure 4). Data from the early 2000s show a notably low occurrence of flood events due to a low volume of news data. Excluding this minimum, the year 2003 emerges as having the least number of flood events. The year 2010 stood out with the highest occurrence of floods, significantly impacting 525 counties. After 2010, excluding the impact of peak values, the overall trend shows a slight increase again.

365 The number of flood-related news reports each month of every year is displayed in Figure 9, showing characteristics similar to the temporal distribution of flood events. The year 2010 was marked by an exceptionally high volume of news, particularly from June through August, and a notable surge in May. July frequently emerges as the month with the highest reportage, emphasizing the heightened flood risk during this period.

4.3.2 Spatial distribution of flood events

370 The spatial distribution of accumulated flood frequency by the county level in China from 2000 to 2022 is shown in Figure 10, whereas the frequency has been classified into 5 levels by the natural breaking method (0–1, 1–5, 5–9, 9–13, 13–22). Level 2 accounts for the largest percentage (50%) followed by Level 1 (29%) and Level 3 (16%), while Levels 3 and 4 are also extremely low (4% and 1%). Most of the county areas in China have experienced flood events. Regions experiencing the most frequent floods include the level 5 and level 4 areas, which are located in the southwest interior of China, such as Sichuan Province;
375 the northwest, including Lanzhou Province; and the southern coastal regions like Guangdong Province, Fujian Province, and Guangxi Province. This pattern is similar to the findings of Liang et al. (2019), whose analysis of historical meteorological data revealed a higher concentration of floods in southern provinces including Guangdong, Hainan, Guangxi, and Fujian.

The province with the most floods was Guangxi, with 960 reported flood events. Guangxi is located in the southwest of China, between 20°54′–26°23′N, 104°29′–112°04′E, in the South Asian tropical monsoon climate zone (Nie et al., 2012; Gao
380 et al., 2020b). The region is characterized by high temperatures, a long summer, short winter, and distinct wet and dry seasons. The annual average temperature is 22.5°C, and the annual average precipitation is 1806 mm (Qiu et al., 2021). Studies indicate

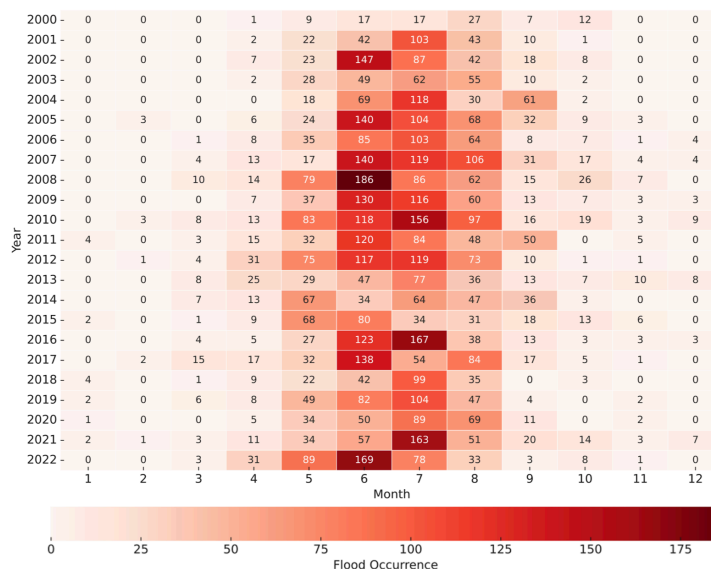


Figure 8. A heat map showing in each cell the number of flood occurrence for each month and each year.

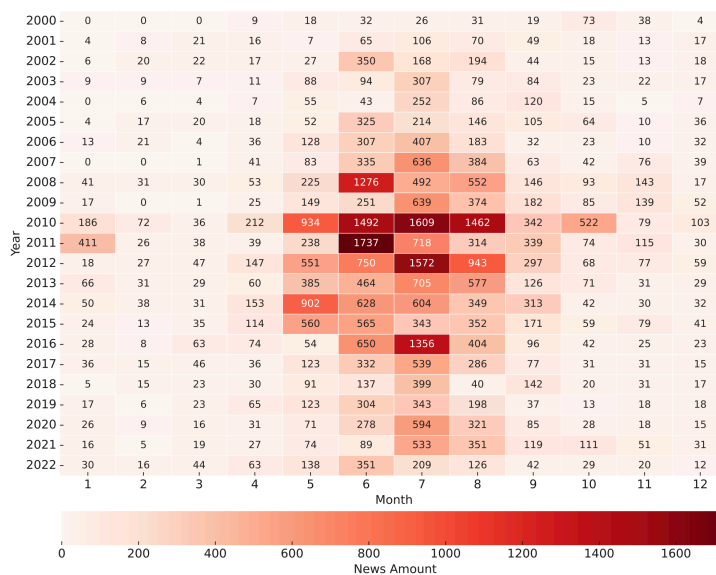


Figure 9. A heat map showing in each cell the number of news reports for each month and each year.

that Guangxi experienced flood disasters caused by heavy rainfall frequently (Li et al., 2023; Ma et al., 2023a). Qin et al. (2021) observed an increase in flood hazards in Guangxi since the 1990s and predicted that future precipitation in the region tends to intensify.



385 To further examine the spatial characteristics of historical flood events in China, an analysis was conducted on the distribution
across various basin divisions and climate zones, using the Theil–Sen estimator for robust trend detection. The Theil–Sen
estimator is a non-parametric method that calculates the slope among points, offering a robust way to track changes in flood
occurrences over time (Kemter et al., 2023). The spatial distribution and trend analysis of flood occurrence within China’s river
basins shown in Figure 11 reveal a distinct pattern: a higher occurrence in the east than in the west, and a higher occurrence in
390 the south compared to the north. The Yangtze River Basin (III) and the Pearl River Basin (V) exhibit a notably higher frequency
of flooding, with 3617 and 1794 events respectively, suggesting a pronounced vulnerability to flooding within these populous
and economically pivotal regions. In contrast, the Continental Basin (I) and the Southwest Basin (II) display a relatively lower
frequency of flood events. Trend directions are also reflected in this figure, symbolically represented by triangles, where the
orientation indicates an increasing or decreasing trend in flood frequency. Notably, although the Yangtze River Basin (III) and
395 the Pearl River Basin (V) exhibit the highest frequency of floods, the overall trend is decreasing, whereas other basins show
different levels of increasing trends. Furthermore, adjacent basins do not necessarily share similar trends; for instance, the
Yellow River Basin (IV) presents a more pronounced increasing trend, whereas the adjacent Huaihe River Basin (VII) exhibits
a nearly zero slope, implying the potential influence of localized environmental or anthropogenic factors.

Figure 12 offers the spatial distribution and trend of flood occurrence concerning China’s diverse climate zones. The sub-
400 tropical zones, specifically the South Subtropical Zone (IV), North Subtropical Zone (V), and Central Subtropical Zone (III),
are characterized by a higher frequency of flooding, with 1336, 1597, and 3222, respectively. These zones, which endure the
bulk of flood events, exhibit contrasting trends. Whereas the South Subtropical Zone (IV) indicates a trend towards an increase
in flood events, the Central Subtropical Zone (III) and the North Subtropical Zone (V) show a slight decrease, highlighting the
non-monotonic nature of flood trends across climatic gradients. In addition, the South Temperate Zone (I) displays a relatively
405 higher frequency and an increasing trend of flood events. Conversely, the North Temperate Zone (VII), the Central Tropical
Zone (IX), and the Plateau Climate Zone (II) experience a minimal frequency of flood events and a near-zero trend coefficient,
suggesting a relatively lower impact of flooding.

5 Discussion

The dataset constructed in this study serves as a supplement to official datasets, particularly in filling the gaps regarding the
410 distribution of flood event distribution at the county level. It offers robust data support for future research on urban flooding,
enabling a detailed understanding of flood dynamics across different areas. Notably, the temporal and spatial distribution
characteristics revealed consistent with the findings of previous studies, offering corroborative evidence on the dynamics of
urban flood events.

The temporal distribution revealed an increasing trend in urban flood events over time when the peak value is excluded
415 from consideration. The increase of urban floods is mainly due to an increase in extreme rainfall events coupled with the rapid
urbanization (Wu et al., 2021; Cheng et al., 2020). On the one hand, urban floods are intensified by changes in precipitation
patterns due to global warming, which increases both the intensity and frequency of rainfall (Kong et al., 2021). Kundzewicz

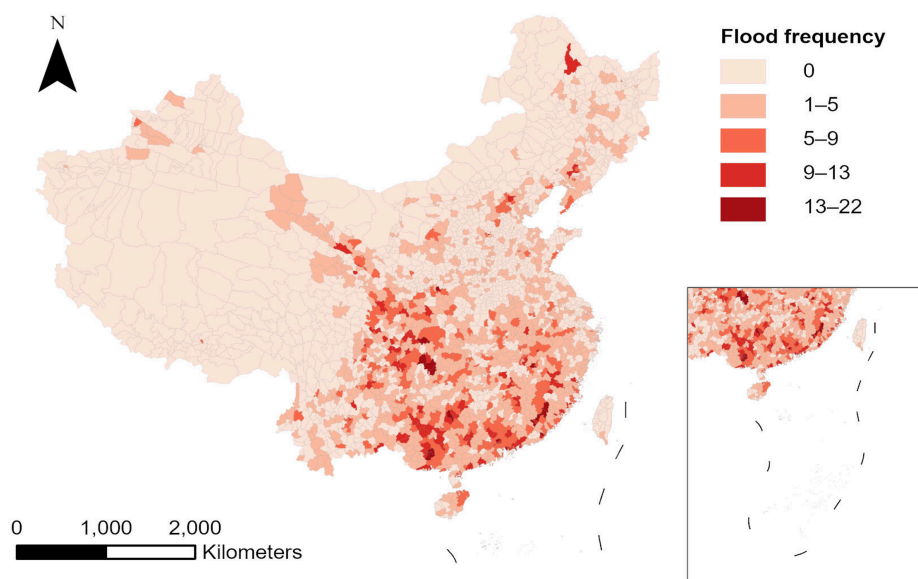


Figure 10. The accumulated flood occurrence by the county level in China from 2000–2022.

et al. (2019) found an increase in the annual number of heavy-rain days (daily precipitation ≥ 50 mm) in China from 1961 to 2017. On the other hand, rapid urbanization in China intensified the imperviousness of urban surfaces leading to the increasing
420 of urban flood risk (Wang et al., 2022; Du et al., 2015). Urbanization leads to changes from natural surfaces such as soil and vegetation to impervious materials like asphalt, which prevents rainfall from effectively seeping into the ground, accelerating the speed of runoff and thus increasing flood risk (Huong and Pathirana, 2013; Luo and Zhang, 2022). Notably, China has been the largest contributor to the global expansion in high-hazard settlements in flood zones, reflecting the impact of its rapid urban growth (Rentschler et al., 2023).

425 Shifting focus to spatial distribution, this paper discusses the flood distribution pattern from two perspectives including basins and climate zones. Overall, the southern and eastern regions of China are more affected by flooding, which is consistent with previous findings in flood risk and peak precipitation distribution (Sun et al., 2024; Gao et al., 2020a). Specifically, the Yangtze and Pearl River basins are the most frequently flooded areas, which is similar to the findings of Fang et al. (2021). The Yangtze and Pearl River basins are two of China's most economically developed and densely populated regions (Pan et al.,
430 2023; Ma et al., 2023b), facing significant environmental challenges due to their vulnerability to extreme rainfall events and associated flood disasters (Yang et al., 2022; Xu et al., 2021). However, our trend analysis indicates a decrease in flood events in both the Yangtze and Pearl River basins, contrasting with Zhou et al. (2017)'s findings of increased extreme rainfall across all cities in the Yangtze Basin. This difference is attributed to the impact of a peak year within our study period, with 2010

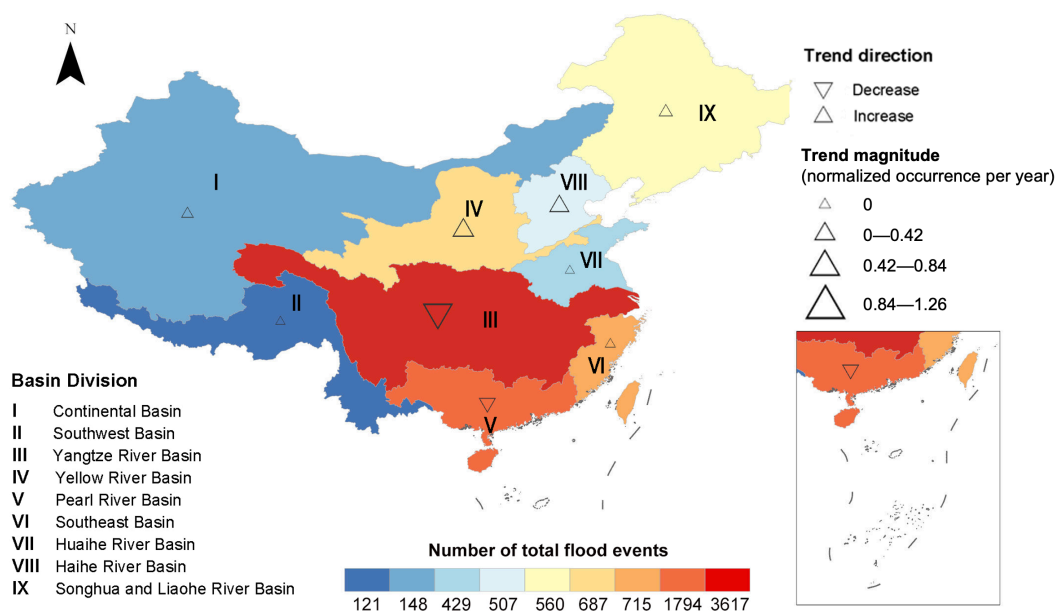


Figure 11. The accumulated flood occurrence and trend in different basins from 2000–2022. Roman numerals are used to represent different basins. Color indicates the number of flood events, with shades closer to red denoting higher occurrence. Triangles indicate trend characteristics, where downward and upward triangles represent decreases and increases, respectively, and the size is used to characterize the value of the slope.

being identified as a significant peak time primarily due to the event count in these river basins. The negative growth trend
435 calculated in this paper needs to be verified by more studies, and it cannot be interpreted as a reduction in flood.

Subtropical regions received the most frequent flood events in this study. Subtropical regions with their high temperatures and high humidity, particularly during summer and autumn, are especially prone to short-term heavy precipitation caused by convective activities (Li et al., 2022; Kotz et al., 2023). These climatic conditions make subtropical zones the primary contributors to the overall flood event count in China.

440 Despite the valuable insights provided by the spatial and temporal analysis in this study, it is crucial to acknowledge the limitations imposed by our reliance on news data, which may introduce systemic errors due to media attention. Future research should aim to integrate other data sources, such as social media and remote-sensing data, to improve the data quality. Furthermore, the subsequent analysis of the extracted information in this present study is limited to the presentation of spatiotemporal distribution, thus failing to highlight the unique value of county-level data in revealing regional flood characteristics. Future
445 research could focus on utilizing the dataset constructed in this present study for more detailed analysis. Attribution analysis of

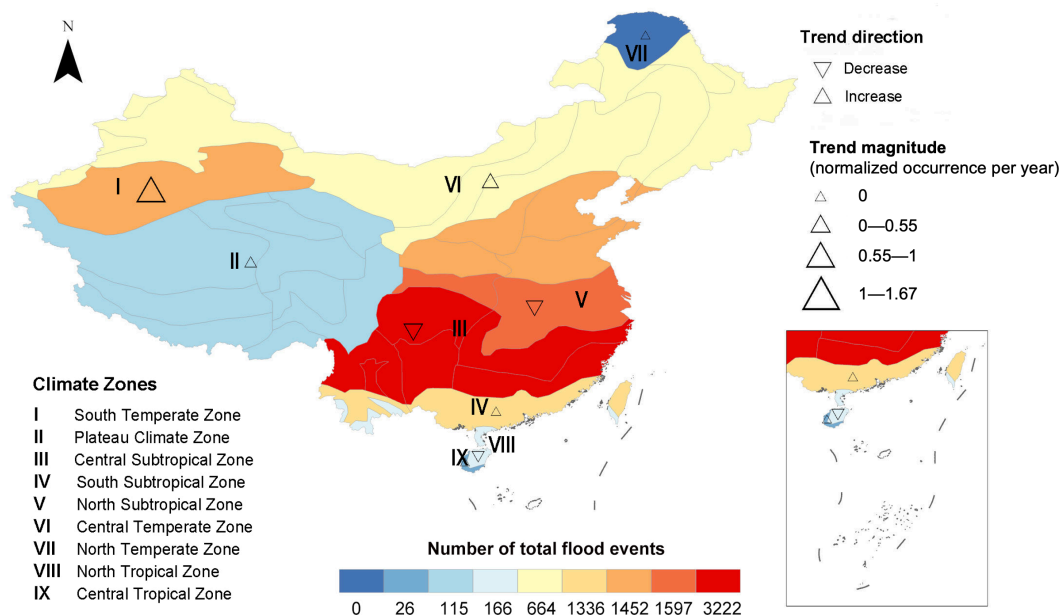


Figure 12. The accumulated flood occurrence and trend in different climate zones from 2000–2022. Roman numerals are used to represent different climate zones. Color indicates the number of flood events, with shades closer to red denoting higher occurrence. Triangles indicate trend characteristics, where downward and upward triangles represent decreases and increases, respectively, and the size is used to characterize the value of the slope.

floods could be studied to explore the main contributing factors in different areas. Additionally, by analyzing changes in land use and urban planning in specific counties, a more comprehensive understanding of how various factors interact at the local level to cause flood events can be achieved.

6 Conclusions

450 This study constructed a national urban flood dataset at the county level in China based on news media data through a question-answer format BERT model, providing an analysis of flood events in China and highlighting their temporal and spatial patterns. The BERT model was initially employed for spatiotemporal information extraction, achieving an F1 score of 0.86 and an exact match score of 0.82. Flood locations were then identified using a named entity recognition model that combines a BiLSTM network with a CRF layer. The established dataset consists of records from 2048 counties affected by flood disasters between



455 2000 and 2022, with a total number of 7559 events. This dataset is hosted on a GitHub repository and will be updated with the latest findings from flood-related news articles, thereby enhancing its utility for future research.

Although lacking authoritative county-level flood distribution data for validation, the initial accuracy of the trend in extracted information was confirmed by comparing the number of flooded cities with those reported in the *China Flood and Drought Bulletin*. Subsequent case studies of two widespread typhoon events established a strong correlation between flood distribution and typhoon paths. Further analysis showed that flood-prone regions are typically in areas with high precipitation and low elevation, aligning with established hydrological principles. These validations confirm the accuracy of the dataset records constructed in this study, which can serve as a supplement to authoritative datasets and provide support for future research on urban floods.

Building on the insights from the flood event sets, this study further examines the temporal and spatial patterns of flood occurrence in China. Temporally, the total flood occurrence from 2000 to 2022, excluding the influence of peak year, shows an upward trend. The peak in flood occurrence is identified in 2010, when 525 counties were affected. In addition, the seasonal characteristics shows that the rainy climate in summer leads to summer floods accounting for 74% of the total, highlighting the importance of being prepared for floods during this period. Spatially, flood occurrence was decreased from southeast to northwest. The southeastern regions like Guangdong Province, Fujian Province, and Guangxi Province and the southwest of interior China like Sichuan Province, are the most frequently flooded areas. The Yangtze River Basin and Pearl River Basin, as economically developed and populated areas, were identified as areas particularly prone to flooding. As for climate zones, most of the subtropical zones across China experienced more floods than other climate zones.

Data availability. The national flood dataset constructed in this present study is accessible on a Github repository (<https://github.com/shengnan0218/China-urban-flood-dataset.git>) and will be continuously updated with new findings from flood-related news articles, enhancing its value for ongoing research. In addition, the DEM data used in this study was downloaded from <http://www.gscloud.cn>. The precipitation was derived from ERA5 data (Hersbach et al., 2020) (<https://cds.climate.copernicus.eu>).

Appendix A: Appendix

Table A1 shows the F1 score values used to evaluate BERT model performance during the hyperparameter tuning process, with a different calculation method from the main text. Precision and recall are calculated as:

$$480 \text{ Precision} = \frac{O}{L} \tag{A1}$$

$$\text{Recall} = \frac{O}{S} \tag{A2}$$



O is defined as the maximum overlapping character length between the model's output and the standard annotated answer, L is the length of the output answer and S is the length of the standard answer. Finally, the F1 score is refer to Formula 3 in Section 3.

Table A1. The performance of BERT model with different hyperparameters during fine-tuning process

Learning rate	Batch size	F1 score
1×10^{-5}	4	83.35
1×10^{-5}	8	81.86
5×10^{-5}	4	83.81
5×10^{-5}	8	84.82

Table A2 shows the annual number of flooded cities in *China Flood and Drought Bulletin* and WiseNews.

Table A2. The comparison between the number of flooded cities in *China Flood and Drought Bulletin* and WiseNews

Year	Number of flooded cities in bulletin	Number of flooded cities in WiseNews
2006	118	116
2007	109	87
2008	115	100
2009	136	125
2010	258	167
2011	136	131
2012	184	141
2013	243	137
2014	125	108
2015	168	113
2016	192	135
2017	104	108
2018	83	96

Author contributions. Shengnan Fu conducted the investigation, developed the methodology, handled coding, and wrote the original draft. Heng Lyu provided guidance on methodology, and reviewed and edited the manuscript. David M. Schultz and Zhonghua Zheng also guided the methodology and coding, respectively, and participated in manuscript editing. Chi Zhang supervised the project and provided funding.



490 *Competing interests.* The authors declare that they have no known competing financial interests or personal relationships that could have appeared to influence the work reported in this paper.

Acknowledgements. This work was supported by several funding sources. The research was funded by. This research was partially supported by the fund of the National Key R&D Program of China (Grant No. 2022YFC3090601), National Science Foundation for Distinguished Young Scholars (Grant No. 51925902), and Key Fund of National Natural Science Foundation of China (Grant No. U2240204). We also
495 thank the China Scholarship Council for supporting Shengnan Fu's studies in Manchester, which facilitated this project. Additionally, David M. Schultz was partially supported by the Natural Environment Research Council UK (Grants NE/W000997/1 and NE/X018539/1).



References

- Ahemaitihali, A. and Dong, Z.: Spatiotemporal Characteristics Analysis and Driving Forces Assessment of Flash Floods in Altay, *Water*, 14, 331, <https://doi.org/10.3390/w14030331>, 2022.
- 500 Antwi, S. H., Rolston, A., Linnane, S., and Getty, D.: Communicating water availability to improve awareness and implementation of water conservation: A study of the 2018 and 2020 drought events in the Republic of Ireland, *Science of The Total Environment*, 807, 150 865, <https://doi.org/https://doi.org/10.1016/j.scitotenv.2021.150865>, 2022.
- Avellaneda, P., Ficklin, D., Lowry, C., Knouft, J., and Hall, D.: Improving hydrological models with the assimilation of crowdsourced data, *Water Resources Research*, 56, e2019WR026 325, <https://doi.org/https://doi.org/10.1029/2019WR026325>, 2020.
- 505 Brooks, H. E., Flora, M. L., and Baldwin, M. E.: A rose by any other name: On basic scores from the 2x2 table and the plethora of names attached to them, *Artificial Intelligence for the Earth Systems*, <https://doi.org/10.1175/AIES-D-23-0104.1>, 2024.
- Bui, Q. C., Campos, D., van Mulligen, E., and Kors, J.: A fast rule-based approach for biomedical event extraction, in: proceedings of the BioNLP shared task 2013 workshop, pp. 104–108, 2013.
- Cao, W., Zhou, Y., Güneralp, B., Li, X., Zhao, K., and Zhang, H.: Increasing global urban exposure to flooding: An analysis of long-term annual dynamics, *Science of The Total Environment*, 817, 153 012, <https://doi.org/https://doi.org/10.1016/j.scitotenv.2022.153012>, 2022.
- 510 Chan, F., Gu, X., Qi, Y., Chen, Y., Lu, X., Li, L., Griffiths, J., Zhu, F., Li, J., and Chen, W.: Lessons learnt from Typhoons Fitow and In-Fa: implications for improving urban flood resilience in Asian Coastal Cities, *Natural Hazards*, 110, <https://doi.org/10.1007/s11069-021-05030-y>, 2021.
- Chen, J., Li, Y., and Zhang, C.: The Effect of Design Rainfall Patterns on Urban Flooding Based on the Chicago Method, *International Journal of Environmental Research and Public Health*, 20, <https://doi.org/10.3390/ijerph20054245>, 2023.
- 515 Cheng, T., Xu, Z., Yang, H., Hong, S., and Leitão, J.: Analysis of Effect of Rainfall Patterns on Urban Flood Process by Coupled Hydrological and Hydrodynamic Modeling, *Journal of Hydrologic Engineering*, 25, 04019 061, [https://doi.org/10.1061/\(ASCE\)HE.1943-5584.0001867](https://doi.org/10.1061/(ASCE)HE.1943-5584.0001867), 2020.
- Cui, Y., Liu, T., Che, W., Xiao, L., Chen, Z., Ma, W., Wang, S., and Hu, G.: A span-extraction dataset for Chinese machine reading comprehension, in: Proceedings of the 2019 Conference on Empirical Methods in Natural Language Processing and the 9th International Joint Conference on Natural Language Processing (EMNLP-IJCNLP), pp. 5883–5889, <https://doi.org/10.18653/v1/D19-1600>, 2018.
- 520 Darabi, H., Haghighi, A. T., Rahmati, O., Shahrood, A. J., Rouzbeh, S., Pradhan, B., and Bui, D. T.: A hybridized model based on neural network and swarm intelligence-grey wolf algorithm for spatial prediction of urban flood-inundation, *Journal of Hydrology*, 603, 126 854, <https://doi.org/https://doi.org/10.1016/j.jhydrol.2021.126854>, 2021.
- 525 Datla, R. V., Kessel, R., Smith, A. W., Kacker, R. N., and Pollock, D. B.: Review Article: Uncertainty analysis of remote sensing optical sensor data: guiding principles to achieve metrological consistency, *International Journal of Remote Sensing*, 31, 867–880, <https://doi.org/10.1080/01431160902897882>, 2010.
- Devlin, J., Chang, M.-W., Lee, K., and Toutanova, K.: Bert: Pre-training of deep bidirectional transformers for language understanding, <https://doi.org/https://doi.org/10.48550/arXiv.1810.04805>, 2018.
- 530 Dong, B., Xia, J., Li, Q., and Zhou, M.: Risk assessment for people and vehicles in an extreme urban flood: Case study of the “7.20” flood event in Zhengzhou, China, *International journal of disaster risk reduction*, 80, 103 205, <https://doi.org/https://doi.org/10.1016/j.ijdr.2022.103205>, 2022.



- Donovan, M., Belmont, P., Notebaert, B., Coombs, T., Larson, P., and Souffront, M.: Accounting for uncertainty in remotely-sensed measurements of river planform change, *Earth-Science Reviews*, 193, 220–236, <https://doi.org/https://doi.org/10.1016/j.earscirev.2019.04.009>,
535 2019.
- Du, S., Wen, J., Shi, P., and Van Rompaey, A.: Quantifying the impact of impervious surface location on flood peak discharge in urban areas, *Natural Hazards*, 76, <https://doi.org/10.1007/s11069-014-1463-2>, 2015.
- Eini, M., Kaboli, H. S., Rashidian, M., and Hedayat, H.: Hazard and vulnerability in urban flood risk mapping: Machine learning techniques and considering the role of urban districts, *International Journal of Disaster Risk Reduction*, 50, 101687,
540 <https://doi.org/https://doi.org/10.1016/j.ijdr.2020.101687>, 2020.
- Fang, J., Zhang, C., Fang, J., Liu, M., and Luan, Y.: Increasing exposure to floods in China revealed by nighttime light data and flood susceptibility mapping, *Environmental Research Letters*, 16, <https://doi.org/10.1088/1748-9326/ac263e>, 2021.
- Farooq, H. et al.: Review of deep learning techniques for improving the performance of machine reading comprehension problem, in: 2020 4th International Conference on Intelligent Computing and Control Systems (ICICCS), pp. 928–935,
545 <https://doi.org/10.1109/ICICCS48265.2020.9121015>, 2020.
- Feng, J., Li, D., Li, Y., and Zhao, L.: Analysis of compound floods from storm surge and extreme precipitation in China, *Journal of Hydrology*, 627, 130402, <https://doi.org/https://doi.org/10.1016/j.jhydrol.2023.130402>, 2023.
- Feng, Y., Xiao, Q., Brenner, C., Peche, A., Yang, J., Feuerhake, U., and Sester, M.: Determination of building flood risk maps from LiDAR mobile mapping data, *Computers, Environment and Urban Systems*, 93, 101759,
550 <https://doi.org/https://doi.org/10.1016/j.compenvurbsys.2022.101759>, 2022.
- Fu, S., Lyu, H., Wang, Z., Hao, X., and Zhang, C.: Extracting historical flood locations from news media data by the named entity recognition (NER) model to assess urban flood susceptibility, *Journal of Hydrology*, 612, 128312, <https://doi.org/https://doi.org/10.1016/j.jhydrol.2022.128312>, 2022.
- Gao, X., Guo, M., Yang, Z., Zhu, Q., Xu, Z., and Gao, K.: Temperature dependence of extreme precipitation over mainland China, *Journal of Hydrology*, 583, 124595, <https://doi.org/https://doi.org/10.1016/j.jhydrol.2020.124595>, 2020a.
555
- Gao, Y., Zhang, Y., Lei, L., and Tang, J.: Multi-scale characteristics of an extreme rain event in Shandong Province, produced by Typhoon Lekima (2019), *Frontiers in Earth Science*, 10, <https://doi.org/10.3389/feart.2022.1093545>, 2023.
- Gao, Z., Huang, B., Ma, Z., Chen, X., Qiu, J., and Liu, D.: Comprehensive comparisons of state-of-the-art gridded precipitation estimates for hydrological applications over southern China, *Remote Sensing*, 12, 3997, <https://doi.org/10.3390/rs12233997>, 2020b.
- 560 Guo, K., Guan, M., and Yu, D.: Urban surface water flood modelling—a comprehensive review of current models and future challenges, *Hydrology and Earth System Sciences*, 25, 2843–2860, <https://doi.org/10.5194/hess-25-2843-2021>, 2021.
- He, W., Liu, K., Liu, J., Lyu, Y., Zhao, S., Xiao, X., Liu, Y., Wang, Y., Wu, H., She, Q., Liu, X., Wu, T., and Wang, H.: DuReader: a Chinese Machine Reading Comprehension Dataset from Real-world Applications, pp. 37–46, <https://doi.org/10.18653/v1/W18-2605>, 2018.
- Hersbach, H., Bell, B., Berrisford, P., Hirahara, S., Horányi, A., Muñoz Sabater, J., Nicolas, J., Peubey, C., Radu, R., Schepers, D., Simmons, A., Soci, C., Abdalla, S., Abellan, X., Balsamo, G., Bechtold, P., Biavati, G., Bidlot, J., Bonavita, M., and Thépaut, J. N.: The ERA5 global reanalysis, *Quarterly Journal of the Royal Meteorological Society*, <https://doi.org/10.1002/qj.3803>, 2020.
- Houston, J. B., Pfefferbaum, B., and Rosenholtz, C. E.: Disaster news: framing and frame changing in coverage of major U.S. natural disasters, 2000–2010, *Journalism & Mass Communication Quarterly*, 89, 606–623, <https://doi.org/10.1177/1077699012456022>, 2012.
- Huang, M. and Jin, S.: Rapid Flood Mapping and Evaluation with a Supervised Classifier and Change Detection in Shouguang Using
570 Sentinel-1 SAR and Sentinel-2 Optical Data, *Remote Sensing*, 12, <https://doi.org/10.3390/rs12132073>, 2020.



- Huang, W., Wu, C., Luo, S., Chen, K., Wang, H., and Toda, T.: Speech recognition by simply fine-tuning BERT, in: ICASSP 2021–2021 IEEE International Conference on Acoustics, Speech and Signal Processing (ICASSP), pp. 7343–7347, 2021.
- Huong, H. T. L. and Pathirana, A.: Urbanization and climate change impacts on future urban flooding in Can Tho city, Vietnam, *Hydrology and Earth System Sciences*, 17, 379–394, <https://doi.org/10.5194/hess-17-379-2013>, 2013.
- 575 Jiang, R., Lu, H., Yang, K., Chen, D., Zhou, J., Yamazaki, D., Pan, M., Li, W., Xu, N., Yang, Y., Guan, D., and Tian, F.: Substantial increase in future fluvial flood risk projected in China’s major urban agglomerations, *Communications Earth & Environment*, 4, <https://doi.org/10.1038/s43247-023-01049-0>, 2023.
- Kemter, M., Marwan, N., Villarini, G., and Merz, B.: Controls on Flood Trends Across the United States, *Water Resources Research*, 59, e2021WR031 673, <https://doi.org/10.1029/2021WR031673>, 2023.
- 580 Kong, F., Sun, S., and Wang, Y.: Comprehensive Understanding the Disaster-Causing Mechanism, Governance Dilemma and Targeted Countermeasures of Urban Pluvial Flooding in China, *Water*, 13, <https://doi.org/10.3390/w13131762>, 2021.
- Kotz, M., Lange, S., Wenz, L., and Levermann, A.: Constraining the Pattern and Magnitude of Projected Extreme Precipitation Change in a Multimodel Ensemble, *Journal of Climate*, 37, <https://doi.org/10.1175/JCLI-D-23-0492.1>, 2023.
- Kundzewicz, Z. W., Su, B., Wang, Y., Xia, J., Huang, J., and Jiang, T.: Flood risk and its reduction in China, *Advances in Water Resources*, 585 130, 37–45, <https://doi.org/https://doi.org/10.1016/j.advwatres.2019.05.020>, 2019.
- Lai, K., Porter, J. R., Amodeo, M., Miller, D., Marston, M., and Armal, S.: A Natural Language Processing Approach to Understanding Context in the Extraction and GeoCoding of Historical Floods, Storms, and Adaptation Measures, *Information Processing & Management*, 59, 102 735, <https://doi.org/10.1016/j.ipm.2021.102735>, 2022.
- Li, R., Jiang, Z., Wang, L., Lu, X., Zhao, M., and Chen, D.: Enhancing Transformer-based language models with Commonsense Representations for Knowledge-driven Machine Comprehension, *Knowledge-Based Systems*, <https://doi.org/10.1016/j.knosys.2021.106936>, 2021.
- 590 Li, X., Yin, F., Sun, Z., Li, X., Yuan, A., Chai, D., Zhou, M., and Li, J.: Entity-Relation Extraction as Multi-Turn Question Answering, in: Proceedings of the 57th Annual Meeting of the Association for Computational Linguistics, pp. 1340–1350, <https://doi.org/10.18653/v1/P19-1129>, 2019.
- Li, Y., Deng, Y., Cheung, H. N., Zhou, W., Yang, S., and Zhang, H.: Amplifying subtropical hydrological transition over China in early summer tied to weakened mid-latitude synoptic disturbances, *npj Climate and Atmospheric Science*, 5, <https://doi.org/10.1038/s41612-022-00259-1>, 2022.
- 595 Li, Z., Tang, X., Li, L., Chu, Y., Wang, X., and Yang, D.: GIS-based risk assessment of flood disaster in the Lijiang River Basin, *Scientific Reports*, 13, <https://doi.org/10.1038/s41598-023-32829-5>, 2023.
- Liang, Y., Wang, Y., Zhao, Y., Lu, Y., and Liu, X.: Analysis and Projection of Flood Hazards over China, *Water*, 11, 1022, <https://doi.org/10.3390/w11051022>, 2019.
- 600 Liu, J., Chen, Y., Liu, K., Bi, W., and Liu, X.: Event Extraction as Machine Reading Comprehension, in: Proceedings of the 2020 Conference on Empirical Methods in Natural Language Processing (EMNLP), pp. 1641–1651, <https://doi.org/10.18653/v1/2020.emnlp-main.128>, 2020.
- Liu, W., Hsieh, T., and Liu, H.: Flood Risk Assessment in Urban Areas of Southern Taiwan, *Sustainability*, 13, <https://doi.org/10.3390/su13063180>, 2021.
- 605 Liu, X., Guo, H., Lin, Y.-r., Li, Y., and Hou, J.: Analyzing spatial-temporal distribution of natural hazards in China by mining news sources, *Natural Hazards Review*, 19, 04018 006, [https://doi.org/10.1061/\(ASCE\)NH.1527-6996.0000291](https://doi.org/10.1061/(ASCE)NH.1527-6996.0000291), 2018.



- Lu, X., Chan, F. K. S., Li, N., Chen, C., Chen, W., and Chan, H. K.: Improving urban flood resilience via GDELT GKG analyses in China's Sponge Cities, *Scientific Reports*, 12, 20317, <https://doi.org/10.1038/s41598-022-24370-8>, 2022.
- 610 Luo, K. and Zhang, X.: Increasing urban flood risk in China over recent 40 years induced by LUCC, *Landscape and Urban Planning*, 219, <https://doi.org/10.1016/j.landurbplan.2021.104317>, 2022.
- Ma, M., Gao, Q., Xiao, Z., Hou, X., Hu, B., Jia, L., and Song, W.: Analysis of public emotion on flood disasters in southern China in 2020 based on social media data, *Natural Hazards*, 118, <https://doi.org/10.1007/s11069-023-06033-7>, 2023a.
- Ma, X., Brookes, J., Wang, X., Han, Y., Ma, J., Li, G., Chen, Q., Zhou, S., and Qin, B.: Water quality improvement and existing challenges in the Pearl River Basin, China, *Journal of Water Process Engineering*, 55, 104184, <https://doi.org/https://doi.org/10.1016/j.jwpe.2023.104184>, 2023b.
- 615 Nie, C., Li, H., Yang, L., Ye, B., Dai, E., Wu, S., Liu, Y., and Liao, Y.: Spatial and temporal changes in extreme temperature and extreme precipitation in Guangxi, *Quaternary International*, 263, 162–171, <https://doi.org/10.1016/j.quaint.2012.02.029>, 2012.
- Olivetti, E. A., Cole, J. M., Kim, E., Kononova, O., Ceder, G., Han, T., Jin, Y., and Hiszpanski, A. M.: Data-driven materials research enabled
620 by natural language processing and information extraction, *Applied Physics Reviews*, 7, 041317, <https://doi.org/10.1063/5.0021106>, 2020.
- Pan, Z., Gao, G., Fu, B., Liu, S., Wang, J., He, J., and Liu, D.: Exploring the historical and future spatial interaction relationship between urbanization and ecosystem services in the Yangtze River Basin, China, *Journal of Cleaner Production*, 428, 139401, <https://doi.org/https://doi.org/10.1016/j.jclepro.2023.139401>, 2023.
- Qi, W., Yong, B., and Gourley, J. J.: Monitoring the super typhoon lekima by GPM-based near-real-time satellite precipitation estimates,
625 *Journal of Hydrology*, 603, 126968, <https://doi.org/10.1016/j.jhydrol.2021.126968>, 2021.
- Qin, N. X., Wang, J. N., Gao, L., Hong, Y., Huang, J. L., and Lu, Q. Q.: Observed trends of different rainfall intensities and the associated spatiotemporal variations during 1958–2016 in Guangxi, China, *International Journal of Climatology*, 41, E2880–E2895, <https://doi.org/https://doi.org/10.1002/joc.6888>, 2021.
- Qiu, H., Hu, B., and Zhang, Z.: Impacts of land use change on ecosystem service value based on SDGs report–Taking Guangxi as an example,
630 *Ecological Indicators*, 133, 108366, <https://doi.org/https://doi.org/10.1016/j.ecolind.2021.108366>, 2021.
- Rajpurkar, P., Zhang, J., Lopyrev, K., and Liang, P.: Squad: 100,000+ questions for machine comprehension of text, arXiv preprint arXiv:1606.05250, <https://doi.org/https://doi.org/10.48550/arXiv.1606.05250>, 2016.
- Rentschler, J., Avner, P., Marconcini, M., Su, R., Strano, E., Vousdoukas, M., and Hallegatte, S.: Global evidence of rapid urban growth in flood zones since 1985, *Nature*, 622, <https://doi.org/10.1038/s41586-023-06468-9>, 2023.
- 635 Sha, L., Liu, J., Lin, C., Li, S., Chang, B., and Sui, Z.: RBPB: Regularization-based pattern balancing method for event extraction, in: *Proceedings of the 54th Annual Meeting of the Association for Computational Linguistics (Volume 1: Long Papers)*, pp. 1224–1234, 2016.
- Shahabi, H., Shirzadi, A., Ghaderi, K., Omidvar, E., AlAnsari, N., Clague, J. J., Geertsema, M., Khosravi, K., Amini, A., Bahrami, S., Rahmati, O., Habibi, K., Mohammadi, A., Nguyen, H., Melesse, A. M., Ahmad, B. B., and Ahmad, A.: Flood Detection and Susceptibility
640 Mapping Using Sentinel-1 Remote Sensing Data and a Machine Learning Approach: Hybrid Intelligence of Bagging Ensemble Based on K-Nearest Neighbor Classifier, *Remote Sensing*, 12, <https://doi.org/10.3390/rs12020266>, 2020.
- Shang, G., Wang, X., Li, Y., Han, Q., He, W., and Chen, K.: Heterogeneity Analysis of Spatio-Temporal Distribution of Vegetation Cover in Two-Tider Administrative Regions of China, *Sustainability*, 15, <https://doi.org/10.3390/su151813305>, 2023.



- Sun, C., Yang, Z., Wang, L., Zhang, Y., Lin, H., and Wang, J.: Biomedical named entity recognition using BERT in the machine reading
645 comprehension framework, *Journal of Biomedical Informatics*, 118, 103 799, <https://doi.org/https://doi.org/10.1016/j.jbi.2021.103799>,
2021.
- Sun, H., Di, Z., Qin, P., Zhang, S., and Lang, Y.: Spatio-temporal variation and dynamic risk assessment of drought and flood disaster (DFD)
in China, *International Journal of Disaster Risk Reduction*, 100, <https://doi.org/10.1016/j.ijdr.2023.104140>, 2024.
- Surampudi, S. and Yarrakula, K.: Mapping and assessing spatial extent of floods from multitemporal synthetic aperture radar images: a case
650 study on Brahmaputra River in Assam State, India, *Environmental Science and Pollution Research*, 27, <https://doi.org/10.1007/s11356-019-06849-6>, 2020.
- Suwaileh, R., Imran, M., Elsayed, T., and Sajjad, H.: Are we ready for this disaster? Towards location mention recognition from crisis tweets,
in: *Proceedings of the 28th international conference on computational linguistics*, pp. 6252–6263, 2020.
- Taylor, W. L.: “Cloze procedure”: A new tool for measuring readability, *Journalism quarterly*, 30, 415–433, 1953.
- 655 Wang, S., Jiao, S., and Xin, H.: Spatio-temporal characteristics of temperature and precipitation in Sichuan Province, Southwestern China,
1960–2009, *Quaternary International*, 286, 103–115, <https://doi.org/https://doi.org/10.1016/j.quaint.2012.04.030>, 2013.
- Wang, S., Wang, Z., Jiang, Y., and Wang, H.: Hierarchical Annotation Event Extraction Method in Multiple Scenarios, *Wireless Communi-
cations and Mobile Computing*, 2021, 1–9, <https://doi.org/https://doi.org/10.1155/2021/8899852>, 2021.
- Wang, X., Kinsland, G., Poudel, D., and Fenech, A.: Urban flood prediction under heavy precipitation, *Journal of Hydrology*, 577, 123 984,
660 <https://doi.org/https://doi.org/10.1016/j.jhydrol.2019.123984>, 2019.
- Wang, Y., Li, C., Liu, M., Cui, Q., Wang, H., LV, J., Li, B., Xiong, Z., and Hu, Y.: Spatial characteristics and driving factors of urban flooding
in Chinese megacities, *Journal of Hydrology*, 613, 128 464, <https://doi.org/https://doi.org/10.1016/j.jhydrol.2022.128464>, 2022.
- Williamson, R.: Authenticity in Newspaper Coverage of Political Leaders’ Responses to Disaster: A Historical Study, *Journalism Studies*,
20, 1511–1527, <https://doi.org/10.1080/1461670X.2018.1527712>, 2019.
- 665 Wu, J., Li, Y., Ye, T., and Li, N.: Changes in mortality and economic vulnerability to climatic hazards under economic development at
the provincial level in China, *Regional Environmental Change*, 19, 125–136, <https://doi.org/https://doi.org/10.1007/s10113-018-1386-7>,
2019.
- Wu, M., Wu, Z., Ge, W., Wang, H., Shen, Y., and Jiang, M.: Identification of sensitivity indicators of urban rainstorm flood disasters: A case
study in China, *Journal of Hydrology*, 599, 126 393, <https://doi.org/https://doi.org/10.1016/j.jhydrol.2021.126393>, 2021.
- 670 Xiang, W. and Wang, B.: A Survey of Event Extraction From Text, *IEEE Access*, 7, 173 111–173 137,
<https://doi.org/10.1109/ACCESS.2019.2956831>, 2019.
- Xiong, R.: Chinese Conference Event Named Entity Recognition Based on BERT-BiLSTM-CRF, in: *Proceedings of the 3rd International
Conference on Big Data Technologies*, pp. 188–191, 2020.
- Xu, F., Zhou, Y., and Zhao, L.: Spatial and temporal variability in extreme precipitation in the Pearl River Basin, China from 1960 to 2018,
675 *International Journal of Climatology*, 42, <https://doi.org/10.1002/joc.7273>, 2021.
- Xu, X. and Tang, Q.: Meteorological disaster frequency at prefecture-level city scale and induced losses in mainland China during 2011–2019,
Natural Hazards, 109, 827–844, <https://doi.org/10.1007/s11069-021-04858-8>, 2021.
- Yan, Z., Guo, X., Zhao, Z., and Tang, L.: Achieving fine-grained urban flood perception and spatio-temporal evolution analysis based on
social media, *Sustainable Cities and Society*, 101, 105 077, <https://doi.org/10.1016/j.scs.2023.105077>, 2024.
- 680 Yang, C., Zhang, H., Li, X., He, Z., and Li, J.: Analysis of spatial and temporal characteristics of major natural disasters in China from 2008
to 2021 based on mining news database, *Natural Hazards*, 118, 1881–1916, <https://doi.org/10.1007/s11069-023-06097-5>, 2023.



- Yang, P., Zhang, S., Xia, J., Zhan, C., Cai, W., Wang, W., Luo, X., Chen, N., and Li, J.: Analysis of drought and flood alternation and its driving factors in the Yangtze River Basin under climate change, *Atmospheric Research*, 270, 106087, <https://doi.org/10.1016/j.atmosres.2022.106087>, 2022.
- 685 Yoon, W., Lee, J., Kim, D., Jeong, M., and Kang, J.: Pre-trained language model for biomedical question answering, in: Joint European Conference on Machine Learning and Knowledge Discovery in Databases, pp. 727–740, Springer, 2019.
- Zhang, C., Xu, T., Wang, T., and Zhao, Y.: Spatial-temporal evolution of influencing mechanism of urban flooding in the Guangdong Hong Kong Macao greater bay area, China, *Frontiers in Earth Science*, 10, <https://doi.org/10.3389/feart.2022.1113997>, 2023a.
- Zhang, N., Yuan, R., Jarvie, S., and Zhang, Q.: Landscape ecological risk of China's nature reserves declined over the past 30 years, *Ecological Indicators*, 156, 111–155, <https://doi.org/https://doi.org/10.1016/j.ecolind.2023.111155>, 2023b.
- 690 Zhang, Y. and Zhang, H.: FinBERT-MRC: Financial Named Entity Recognition Using BERT Under the Machine Reading Comprehension Paradigm, *Neural Processing Letters*, 55, 1–21, <https://doi.org/10.1007/s11063-023-11266-5>, 2023.
- Zhang, Y., Xia, J., Yu, J., Randall, M., Zhang, Y., Zhao, T., Pan, X., Zhai, X., and Shao, Q.: Simulation and assessment of urbanization impacts on runoff metrics: insights from landuse changes, *Journal of Hydrology*, 560, 247–258, <https://doi.org/https://doi.org/10.1016/j.jhydrol.2018.03.031>, 2018.
- 695 Zhang, Z., Jian, X., Chen, Y., Huang, Z., Liu, J., and Yang, L.: Urban waterlogging prediction and risk analysis based on rainfall time series features: A case study of Shenzhen, *Frontiers in Environmental Science*, 11, <https://doi.org/10.3389/fenvs.2023.1131954>, 2023c.
- Zhao, G., Pang, B., Xu, Z., Yue, J., and Tu, T.: Mapping flood susceptibility in mountainous areas on a national scale in China, *Science of the Total Environment*, 615, 1133–1142, <https://doi.org/https://doi.org/10.1016/j.scitotenv.2017.10.037>, 2018.
- 700 Zhou, C., Chen, P., Yang, S., Zheng, F., Yu, H., Tang, J., Lu, Y., Chen, G., Lu, X., Zhang, X., and Sun, J.: The impact of Typhoon Lekima (2019) on East China: a postevent survey in Wenzhou City and Taizhou City, *Frontiers of Earth Science*, 16, 109–120, <https://doi.org/10.1007/s11707-020-0856-7>, 2022.
- Zhou, X., Bai, Z., and Yang, Y.: Linking trends in urban extreme rainfall to urban flooding in China, *International Journal of Climatology*, 37, 4586–4593, <https://doi.org/10.1002/joc.5107>, 2017.
- 705 Zhu, S., Li, D., Feng, H., and Zhang, N.: The influencing factors and mechanisms for urban flood resilience in China: From the perspective of social-economic-natural complex ecosystem, *Ecological Indicators*, 147, 109–959, <https://doi.org/https://doi.org/10.1016/j.ecolind.2023.109959>, 2023.